

Effects of Quinidine on Short QT Syndrome Variant 2 in the Human Ventricle: A Modelling and Simulation Study

Cunjin Luo^{1,2}, Kuanquan Wang¹, Yang Liu¹, Yong Xia³, Henggui Zhang^{1,2,4,5}

¹ School of Computer Science and Technology, Harbin Institute of Technology, Harbin, China

² Key Laboratory of Medical Electrophysiology, Ministry of Education, Collaborative Innovation Centre for Prevention and Treatment of Cardiovascular Disease/Institute of Cardiovascular Research, Southwest Medical University, Luzhou, China

³ School of Computer Science and Technology, Harbin Institute of Technology, Weihai, China

⁴ Space Institute of Southern China, Shenzhen, China

⁵ School of Physics and Astronomy, The University of Manchester, Manchester, United Kingdom

Abstract

The short QT syndrome (SQTS) is a rare cardiac disorder associated with an abnormally short QT interval and an increased risk of ventricular arrhythmias and sudden cardiac death (SCD). Gain-of-function mutation to potassium channels mediating the slow delayed rectifier current, I_{Ks} , underlie KCNQ1-linked SQTS variant 2 (SQT2), in which treatment with sodium, calcium and potassium channel blocking class Ia anti-arrhythmic agents has demonstrated some efficacy. This study used computational modelling and simulation to gain mechanistic insights into the actions the clinical drug, quinidine, in the setting of SQT2. The ten Tusscher et al. human ventricle model was modified to incorporate KCNQ1 V307L mutation-induced changes to I_{Ks} based on experimentally observed data: wild type (WT) and SQT2 mutant conditions were studied. Actions of quinidine were simulated by implementing a simple pore block theory to simulate the drug blocking effects on I_{Kr} , I_{Ks} , I_{to} , I_{Na} , I_{CaL} , I_{NaCa} and I_{NaL} , which were modelled using IC_{50} and Hill coefficient. Cell models were incorporated into one-dimensional (1D) model that considered the intrinsic electrical heterogeneity in the left ventricle. At a clinically therapeutic concentration of $10\mu\text{M}$ quinidine, the action potential duration (APD) was significantly increased, and the QT interval on the pseudo-ECG was prolonged. This study helps to better understand the underlying mechanisms of pharmacological therapy, and provides further evidence that quinidine is a suitable treatment for the SQT2 phenotype.

1. Introduction

The short QT syndrome (SQTS) is a cardiac disorder associated with abnormally short QT interval on the ECG,

leading to increased risk of ventricular arrhythmias and sudden cardiac death (SCD) [1]. The SQTS is genetically heterogeneous, with a complex genotype-phenotype relationship. The SQT2 identified form of the SQTS was caused by a g919c substitution in KCNQ1 encoding the potassium channel. Functional studies of the KCNQ1 V307L mutation revealed a pronounced shift of the half-activation potential and an acceleration of the activation kinetics leading to a gain of function in I_{Ks} , which significantly reduces the QT interval of 290 ms (QTc, 302 ms) [2].

The current first-line treatment for SQTS patients is use of an implantable cardioverter-defibrillator (ICD) device, which protects against SCD [3]. However, the use of ICD device carries an increased risk of an inappropriate shock discharge by the ICD due to T-wave over-sensing. Furthermore, ICD does not restore the QT interval and, is not particularly suited to some pediatric patients, necessitating the pursuance of alternative, pharmacological approaches. Pharmacological therapy may be the primary modality to restore the physiological (normal) QT interval and protect against arrhythmias. At present, the accurate experimental models of SQT2 and in vitro pharmacological data on SQT2 patients are comparatively sparse. However, several studies have reported on the effectiveness of quinidine at restoring the QT interval in the setting of SQTS, as well as on the lack of effect of other anti-arrhythmic agents such as sotalol, ibutilide, and flecainide [4].

Our group recent studies [5,6] adopted computational a modelling and simulation approach to investigate the underlying mechanisms by which combined ion channel blocking actions of quinidine exert anti-arrhythmic effects in the setting of SQTS. Whereas, our group study [7] has previously used computer models to gain insights into QT interval shortening and pro-arrhythmic effects of

SQT2 KCNQ1 V307L mutant I_{Ks} channels in human ventricles, significantly less is known about the pharmacological effects of anti-arrhythmic agents on SQT2. Although the effectiveness of quinidine has only been demonstrated in SQT1, there is a reason to believe that it may be useful in SQT2. Therefore, the present study was undertaken to gain mechanistic information regarding the actions of quinidine on human ventricular electrophysiology in the setting of V307L-linked SQT2.

2. Methods

2.1. Model development

The ten Tusscher et al. model [8] of the human ventricular action potential (AP) was used for simulations in this study, due to its extensive experimental validation and ability to reproduce complex behaviours such as re-entrant excitation waves – a crucial requirement when simulating anti-arrhythmic effects of pharmacological agents on cardiac electrophysiology. Specifically, the single cell AP model can be modelled by using the following ordinary differential equation (ODE):

$$\frac{dV_m}{dt} = -\frac{I_{ion} + I_{stim}}{C_m} \quad (1)$$

where t is time, C_m is the cell membrane capacitance per unit surface area, I_{stim} is the external stimulus current and I_{ion} is the sum of the known transmembrane ionic currents. Particularly, the late sodium current (I_{NaL}) equation [9] was incorporated. The model code used in this study was downloaded from <http://www-binf.bio.uu.nl/khwjtuss/>. The cell model was paced with an amplitude of -52 pA/pF for 1 ms and a basic cycle length (BCL) of 800 ms.

Parameters in the equations for I_{Ks} were modified to incorporate experimental data of Bellocq et al. on SQT2 KCNQ1 V307L mutation-induced changes in I_{Ks} kinetics [2]. The I_{Ks} formulation is described by:

Original:

$$I_{Ks} = G_{Ks} x_s^2 (V_m - E_K) \quad (2)$$

$$x_{s\infty} = \frac{1}{1 + e^{(-5-V_m)/14}} \quad (3)$$

$$\alpha_{xs} = \frac{1400}{\sqrt{1 + e^{(5-V_m)/6}}} \quad (4)$$

$$\beta_{xs} = \frac{1}{1 + e^{(V_m-35)/15}} \quad (5)$$

$$\tau_{xs} = \alpha_{xs} \beta_{xs} + 80 \quad (6)$$

where G_{Ks} is maximal channel conductance, x_s is the activation variable, V_m is the transmembrane potential, E_K is the equilibrium potential, and τ_{xs} is the time constant.

Wild type (WT):

$$x_{s\infty} = \frac{1}{1 + e^{(-5.9-V_m)/17.4}} \quad (7)$$

$$\tau_{xs} = 1 * (\alpha_{xs} \beta_{xs} + 80) \quad (8)$$

Heterozygous mutant expression (Het)

$$x_{s\infty} = \frac{1}{1 + e^{(-20.62-V_m)/10.96}} \quad (9)$$

$$\tau_{xs} = 0.7 * (\alpha_{xs} \beta_{xs} + 80) \quad (10)$$

Homozygous mutant expression (Hom)

$$x_{s\infty} = \frac{1}{1 + e^{(-24.05-V_m)/16.09}} \quad (11)$$

$$\tau_{xs} = 0.52 * (\alpha_{xs} \beta_{xs} + 80) \quad (12)$$

Homozygous mutant expression with reduced I_{Ks} (Homred)

$$x_{s\infty} = \frac{1}{1 + e^{(-24.05-V_m)/16.09}} \quad (13)$$

$$\tau_{xs} = 0.32 * (\alpha_{xs} \beta_{xs} + 80) \quad (14)$$

A scaling factor ratio of 1.5: 1 in epicardial (EPI) I_{Ks} to mid-myocardial (MIDDLE) I_{Ks} , was applied as reported in the study of Szabo et al. [10], in order to generate a high, symmetrical T-wave on the pseudo-ECG of SQTs.

2.2. Drug modelling

A simple pore block theory [11] was used for drug modelling. The effects of quinidine on I_{Kr} , I_{Ks} , I_{to} , I_{Na} , I_{CaL} , I_{NaCa} , and I_{NaL} were described using Hill coefficient (nH) and half maximal inhibitory concentration (IC_{50}) values taken from the literature. The blocking potency of the drug on ionic currents is shown in Table 1. The therapeutic concentration of quinidine is 3.8~10.2 μ M. Therefore, in this study 10 μ M was selected to simulate and predict the effects of quinidine on SQT2.

Table 1. Cardiac ion currents and conductivities (% of original value) in the presence of 10 μ M quinidine.

Current	IC_{50}	nH	Conductivity	Source
I_{Kr}	0.62	0.93	7%	[12]
I_{Ks}	---	---	45.2%	[13]
I_{to}	3.9	1	25.3%	[14]
I_{Na}	0.17	1	59.3%	[15]
I_{CaL}	14.9	1.1	61.2%	[16]
I_{NaCa}	---	---	86.5%	[16]
I_{NaL}	12	1	52.3%	[9]

2.3. Tissue Simulation

Initiation and conduction of action potentials (APs) in the multicellular tissue can be described by the following

partial differential equation (PDE):

$$C_m \frac{\partial V_m}{\partial t} = -(I_{ion} + I_{stim}) + \nabla \cdot (D \nabla V_m) \quad (15)$$

where ∇ is the gradient operator defined within the tissue geometry, D is the diffusion coefficient.

For one-dimensional (1D) simulations, a strand model was 15 mm and employed a spatial resolution of 0.15 mm, close to the ventricular cell length of 80~150 μm . The strand had 25 nodes for ENDO, 35 nodes for MIDDLE and 40 nodes for EPI cells. The total length and proportion for each sub-region reliably reproduced a positive T wave on the pseudo-ECG. D was set at 0.0008 cm^2/ms , which promoted a conduction velocity (CV) of 52 cm/s , close to the experimental CV of ~50 cm/s .

A pseudo-ECG was calculated by the following expression [17]:

$$\phi_e(x') = \frac{\alpha^2}{4} \int (-\nabla V_m) \cdot \nabla \left(\frac{1}{r}\right) dx \quad (16)$$

where α is the radius of the 1D strand, dx is the spatial resolution, r is the Euclidean distance from a strand point x to the electrode point x' . The virtual electrode was placed at a position 2.0 cm away from the EPI end of the strand.

3. Results

Figure 1 shows the simulated ENDO, MIDDLE and EPI cell action potentials and I_{Ks} profile with the modified I_{Ks} equations. These plots show cell action potential V (mV) versus time t (ms), stimulated by a 1.25 Hz frequency. The I_{Ks} in the WT condition increased progressively, however, in the SQT2 conditions, I_{Ks} increased more rapidly, and reached a higher peak amplitude, leading to the shortening of the action potential duration. This results indicate that the modified model can capture the features of the WT and mutant I_{Ks} channel dynamics, and suggest that it can be used to predict the effects of quinidine on SQT2.

The effects of 10 μM quinidine on the cell action potentials are shown in Figure 2. The results indicate that quinidine markedly decreased the action potential amplitude and prolonged the action potential duration in SQT2 conditions. A pseudo-ECG was simulated by using a 1D strand model as shown in Figure 3. The QT interval on the ECG was prolonged in SQT2 conditions by the application of 10 μM quinidine. Especially, the QT interval in the simulated dose of quinidine under the Het condition was prolonged to the normal physiological range of QT interval between 363 and 421 ms.

4. Conclusion

In the present study, we have showed that 10 μM quinidine produced a therapeutic effect on ventricular

electrophysiology in SQT2 conditions. This study provides new evidence that quinidine may be a potential pharmacological agent for treating the KCNQ1-linked SQT2 patients.

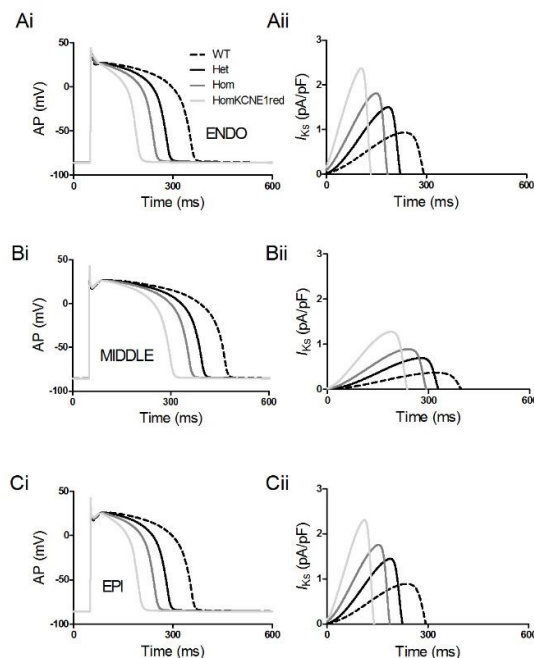


Figure 1. Simulations of ENDO, MIDDLE and EPI cell action potentials together with the corresponding time course of I_{Ks} in WT and SQT2 conditions.

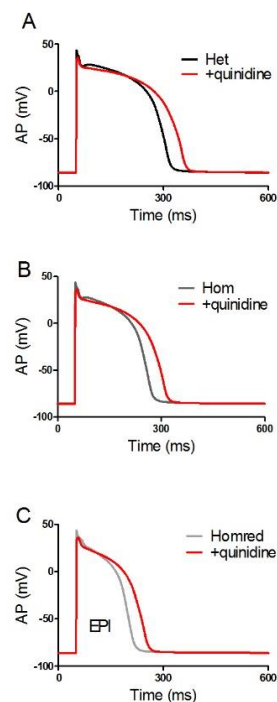


Figure 2. The pharmacological effects of quinidine on cell action potentials in SQT2 conditions.

Acknowledgements

The authors thank Dr. Ismail Adeniran for useful discussions. This study was supported by the China Scholarship Council (CSC), the National Science Foundation of China (NSFC) under Grants No. 61571165 and No. 61572152, and Shandong Province Natural Science Foundation under Grant No. ZR2015FM028.

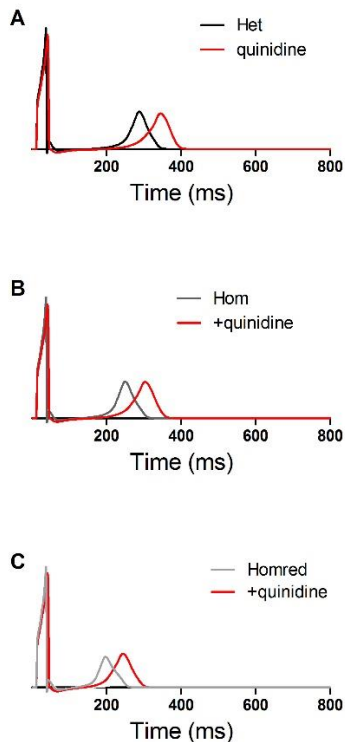


Figure 3. The pharmacological effects of quinidine on pseudo-ECGs in SQT2 conditions.

References

1. Gussak I, Brugada P, Brugada J, Wright RS, Kopecky SL, et al. (2000) Idiopathic short QT interval: a new clinical syndrome? *Cardiology* 94: 99-102.
2. Bellocq C, van Ginneken AC, Bezzina CR, Alders M, Escande D, et al. (2004) Mutation in the KCNQ1 gene leading to the short QT-interval syndrome. *Circulation* 109: 2394-2397.
3. Schimpf R, Wolpert C, Bianchi F, Giustetto C, Gaita F, et al. (2003) Congenital short QT syndrome and implantable cardioverter defibrillator treatment: inherent risk for inappropriate shock delivery. *J Cardiovasc Electrophysiol* 14: 1273-1277.
4. Gaita F, Giustetto C, Bianchi F, Schimpf R, Haissaguerre M, et al. (2004) Short QT syndrome: pharmacological treatment. *J Am Coll Cardiol* 43: 1494-1499.
5. Luo C, Wang K, Zhang H (2017) Modelling the effects of quinidine, disopyramide, and E-4031 on short QT

6. Luo C, Wang K, Zhang H (2017) In silico assessment of the effects of quinidine, disopyramide and E-4031 on short QT syndrome variant 1 in the human ventricles. *PLoS One* 12: e0179515.
7. Zhang H, Kharche S, Holden AV, Hancox JC (2008) Repolarisation and vulnerability to re-entry in the human heart with short QT syndrome arising from KCNQ1 mutation--a simulation study. *Prog Biophys Mol Biol* 96: 112-131.
8. ten Tusscher KH, Panfilov AV (2006) Alternans and spiral breakup in a human ventricular tissue model. *Am J Physiol Heart Circ Physiol* 291: H1088-1100.
9. O'Hara T, Virag L, Varro A, Rudy Y (2011) Simulation of the undiseased human cardiac ventricular action potential: model formulation and experimental validation. *PLoS Comput Biol* 7: e1002061.
10. Szabo G, Szentandrássy N, Biro T, Toth BI, Czifra G, et al. (2005) Asymmetrical distribution of ion channels in canine and human left-ventricular wall: epicardium versus midmyocardium. *Pflügers Arch* 450: 307-316.
11. Brennan T, Fink M, Rodriguez B (2009) Multiscale modelling of drug-induced effects on cardiac electrophysiological activity. *Eur J Pharm Sci* 36: 62-77.
12. McPate MJ, Duncan RS, Hancox JC, Witchel HJ (2008) Pharmacology of the short QT syndrome N588K-hERG K⁺ channel mutation: differential impact on selected class I and class III antiarrhythmic drugs. *Br J Pharmacol* 155: 957-966.
13. Yang T, Kanki H, Zhang W, Roden DM (2009) Probing the mechanisms underlying modulation of quinidine sensitivity to cardiac I(Ks) block by protein kinase A-mediated I(Ks) phosphorylation. *Br J Pharmacol* 157: 952-961.
14. Slawsky MT, Castle NA (1994) K⁺ channel blocking actions of flecainide compared with those of propafenone and quinidine in adult rat ventricular myocytes. *J Pharmacol Exp Ther* 269: 66-74.
15. Koumi S, Sato R, Hayakawa H, Okumura H (1991) Quinidine blocks cardiac sodium current after removal of the fast inactivation process with chloramine-T. *J Mol Cell Cardiol* 23: 427-438.
16. Zhang YH, Hancox JC (2002) Mode-dependent inhibition by quinidine of Na⁺-Ca²⁺ exchanger current from guinea-pig isolated ventricular myocytes. *Clin Exp Pharmacol Physiol* 29: 777-781.
17. Gima K, Rudy Y (2002) Ionic current basis of electrocardiographic waveforms: a model study. *Circ Res* 90: 889-896.

Address for correspondence.

Name: Cunjin Luo

Full postal address: Room 306, Integrated Laboratory Building, School of Computer Science and Technology, Harbin Institute of Technology, Xidazhi Street, Nangang District, Harbin, 150001, China.

E-mail address: cunjin.luo@yahoo.co.uk